Research Square

Preprints are preliminary reports that have not undergone peer review.
They should not be considered conclusive, used to inform clinical practice,
or referenced by the media as validated information.

Exploring the Therapeutic Potential of Momordica charantia in Targeting Protein Kinase C Delta (PRKCD) for Type 2 Diabetes Mellitus: Insights from Network Pharmacology, Molecular Docking, and Molecular Dynamics Simulations

Ruchi Yadav
Nirma University
Nidhi Nambiar
Nirma University
Manushi Shah
Nirma University
Bhumika Patel
bhumika.patel@nirmauni.ac.in
Nirma University

Research Article

Keywords: T2DM, PRKCD, Karela, Momordicoside C, Momorcharaside B, Network Pharmacology, Molecular Docking, MD Simulation

Posted Date: February 5th, 2025

DOI: https://doi.org/10.21203/rs.3.rs-5948998/v1

License: This work is licensed under a Creative Commons Attribution 4.0 International License. Read Full License

Additional Declarations: No competing interests reported.

Version of Record: A version of this preprint was published at In Silico Pharmacology on July 7th, 2025. See the published version at https://doi.org/10.1007/s40203-025-00385-7.

Abstract

Type 2 diabetes mellitus (T2DM) is a chronic condition caused by decreased insulin production and increased insulin resistance, and its prevalence has increased by 49% since 1990. Current treatments for T2DM include pharmacological agents and lifestyle modifications, but they are limited by their side effects and cost. Herbal remedies and natural products have become popular alternative treatments for T2DM as they are associated with fewer side effects. Momordica charantia Linn. (bitter melon) is a member of the Cucurbitaceae family and has been used as a traditional anti-diabetic remedy in various countries for many years. The plant contains several biologically active compounds, including glycosides, saponins, alkaloids, triterpenes, proteins, and steroids. The hypoglycemic activity of Momordica charantia is primarily attributed to its saponins, which are collectively known as charantins, and alkaloids.

Through network pharmacology, Molecular docking and MD simulation we found underlying, mechanism of karela in the treatment of T2DM. Through network pharmacology from 49 targets we found the Protein kinase C delta (PRKCD) as a hub gene. Various studies have also indicated the pathophysiological role of PRKCD in the development of T2DM. Gene expression analysis in 24 patients revealed an overexpression of PRKCD in both prediabetic and diabetic patients. Molecular docking data identified the top three active constituents of karela as Momordicoside C, Momorcharaside B, and Momordin I, with docking scores of -8.0 kcal/mol, -7.9 kcal/mol, and − 7.9 kcal/mol, respectively. Additionally,MD simulation was performed using the GROMACS software and we found that Momordicoside C and Momorcharaside B has good stability and also formed the H-bond at end of the 100ns of simulation. This study revelled new mechanism action of a well-known plant karela in the treatment of T2DM.

1. Introduction

Diabetes mellitus is a serious metabolic disease that affects human health. There are three types of diabetes: type 1 diabetes mellitus (T1DM), type 2 diabetes mellitus (T2DM), and gestational diabetes mellitus (GDM) [1, 2]. T2DM is a chronic condition caused by decreased insulin production and increased insulin resistance and is prevalent worldwide, with a 49% increase since 1990. In 2019, there were 437.9 million reported cases of T2DM, primarily in low- and middle-income countries [3]. T2DM is associated with metabolic diseases such as obesity and increases the risk of heart disease, which is the leading cause of death globally[4]. Currently, mainstream treatments for T2DM include pharmacological agents and lifestyle modification, but these are limited by side effects and cost [5]. Natural products, such as herbal remedies, have become an increasingly popular alternative treatment for T2DM as they have fewer side effects and low cost. The use of natural substances for the treatment of diabetes is considered a promising strategy that may provide solutions for the limitations of current treatments [6, 7].

Plants and their products play a crucial role in nutrition by providing essential nutrients and aiding in the prevention of various illnesses, ultimately enhancing the quality of life worldwide. Traditional plant-based medicines have been used for centuries, but it is important to standardize them to evaluate their potential benefits [8]. The Momordica charantia is widely popular plant in India. Commonly it is known as “bitter melon” and in Hindi as “karela”. This plant belongs to family Cucurbitaceae [9]. Traditionally, bitter melon has been known for its potent antidiabetic, anticancer, anti-inflammatory, antiviral and cholesterol-lowering medicinal properties [10, 11]. The plant contains several biologically active compounds, including glycosides, saponins, alkaloids, triterpenes, proteins, and steroids. The hypoglycemic activity of Momordica charantia is primarily attributed to its saponins, collectively known as charantins, and alkaloids. These saponins have been shown to lower blood glucose levels in both animal studies and clinical trials. Additionally, several phytochemicals isolated from the plant, such as charantins, polypeptide-p, momordin Ic, oleanolic acid 3-O-monodesmoside, and oleanolic acid 3-O-glucuronide, have been found to exhibit hypoglycemic activity. These compounds enhance insulin secretion, increase glucose uptake, and reduce glucose production in the liver. Overall, the presence of various bioactive compounds in Momordica charantia makes it a promising natural remedy for diabetes management [12, 13]. However, due to the presence of multiple compounds and multiple targets in Karela, its underlying mechanism has not been thoroughly explored. In present study we explored the anti-diabetic mechanism of this plant by using a network pharmacology study and validated

through molecular docking and molecular dynamic (MD) simulation study. The network pharmacology study is emerging computational technique for drug discovery and development. Initially, the bioactive compounds of Karela were screened, and the overlapping targets between Karela and T2DM were identified. Protein-protein interaction (PPI) networks and core targets were then established through network topological structure analysis. Gene Ontology (GO) and Kyoto Encyclopedia of Genes and Genomes (KEGG) enrichment analyses were conducted to determine the functions and pathways associated with the overlapping targets. Lastly, molecular docking and molecular dynamic (MD) simulations were performed to evaluate the compound-target binding affinity based on the network pharmacology results. The study outcome aids the identification of novel possible targets of plant constituents and enrichment pathways against T2DM.

2. Material and Methods

2.1 Network Pharmacology

2.1.1 Compound mining and target predictions of active constituents of karela

Active compounds from Momordica charantia L. were chosen by conducting a literature survey, and their SMILES were subsequently downloaded using PubChem (https://pubchem.ncbi.nlm.nih.gov/). BindingDB [14] (https://www.bindingdb.org/rwd/bind/index.jsp) and SwissTargetPrediction (STP) [15] (https://www.swisstargetprediction.ch/) were explored against these active compounds to predict their respective target genes focusing on a "*homo sapiens*" keyword.

2.1.2 Collection of T2DM targets

T2DM related targets were searched using keywords' "diabetes", "diabetes mellitus", type 2 diabetes mellitus", "insulin-independent diabetes", "diabetes mellitus type 2" in databases such as DisGeNET (https://disgenet.com/) [16], Therapeutic Target Database (https://db.idrblab.net/ttd/) [17] and Open Target (https://www.opentargets.org/) [18]. The target names were matched to their corresponding UniProt IDs (https://www.uniprot.org/) [19]. Venny 2.1 (https://bioinfogp.cnb.csic.es/tools/venny/) [20] was utilized to identify overlapping targets from all three databases. The common targets of T2DM, retrieved from three databases, and the identified targets of active compounds of Karela, obtained from SwissTargetPrediction and BindingDB databases, were uploaded into Venny 2.1 to create a Venn diagram showing the overlap between T2DM targets and the targets of Karela's active constituents. The intersection of targets from this Venn diagram was then used for further studies.

2.1.3 PPI Network of Intersected Gene

To further investigate the mechanism of action of active constituents of karela in the treatment of T2DM, the intersection of 49 targets was imported into String. Protein-protein interactions were analysed using String ver. 11.0 (https://string-db.org/) [21]. The minimum combined score was set to 0.9 and protein-protein-interaction (PPI) relationships for "*Homo sapiens"* were obtained. Targets without interaction were removed and the data were saved as SIF files. Next, the PPI network was constructed by importing node1 and node2 into Cytoscape [22]. Finally, the core targets were screened by cluster analysis using the MCODE [23], CytoHubba [24] and CytoNCA [25] plugin of Cytoscape.

2.1.4 GO and KEGG Enrichment Analysis

The GO enrichment analysis was conducted through the utilization of the DAVID (Database for Annotation, Visualization and Integrated Discovery) (https://david.ncifcrf.gov/tools.jsp) database [26]. The Biological Process (BP), Cellular Component (CC), and Molecular Function (MF) modules were chosen and significant biological annotations ($p < 0.05$) were selected for analysis. Additionally, KEGG pathway [27] enrichment analysis was conducted to identify the principal signaling pathways

involved in T2DM using the DAVID database and the graph for KEGG and GO plotted by using SRPLOT(https://bioinformatics.com.cn/en) [28].

2.1.5 Different Gene Expression Analysis

Through network analysis of 49 predicted targets, Protein Kinase C Delta Type (PRKCD) was identified as a hub gene. To determine whether this target is involved in the pathophysiology of T2DM, gene expression analysis was performed using the GEO database. In this database, term “PRKCD” was searched along with “*Homo sapiens”* as filer under species tab. The GSE26168 dataset (https://www.ncbi.nlm.nih.gov/geo/geo2r/?acc=GSE26168&platform=GPL6883) was selected, and GEO2R analysis was performed to download the data. This study involved 24 participants, including 8 controls, 7 with impaired fasting glucose, and 9 with T2DM. PRKCD levels in the blood were analyzed in these groups.

2.2 Prediction of Binding Pocket

In this study, PRKCD was identified as a hub gene through network analysis. However, it does not have a native ligand in the PDB. Therefore, prior to molecular docking, the binding pockets were identified using the CastpFold server (https://cfold.bme.uic.edu/castpfold/), which provides detailed information on the topological and geometrical features, as well as pocket details, of the uploaded protein [29]. Additionally, the PocketDepth server (http://proline.physics.iisc.ernet.in/pocketdepth/), a computational tool for identifying binding pockets in protein structures, was utilized [30].

2.3 Molecular Docking

Molecular docking is a computational method used to study the interactions between a protein and a ligand [31]. Initially, all compounds of Karela were searched for in the PubChem database, and the structures were exported in 3D ‘mol2’ format. Subsequently, the 3D structure of the core protein Protein Kinase C Delta Type (PRKCD) (PDB ID: 1YRK, 1.7Å) was downloaded from the Protein Data Bank (https://www.rcsb.org/). The processes of dehydration, hydrogenation, and charge editing were performed using AutoDock software 4.2.6, resulting in the export of modified protein and compounds as PDBQT files. Docking was performed using AutoDock Vina software 1.2.0 [32]. Finally, the docking results were analyzed and visualized using Discovery Studio Visualizer v21.1.020298.

2.4 MD Simulation

Molecular dynamics (MD) simulation using GROMACS 2022.6 (https://manual.gromacs.org/2022-current/index.html) [33] was employed to model the dynamic process of protein-ligand interactions which aided in validating the precision of drug design and supported the rationale of present study. The protein topology files were generated using the OPLS force field (Optimized Potential for Liquid Simulations, version 15) with the 'pdb2gmx' command. Ligand files for GROMACS were prepared using the external LigParagen web server (https://traken.chem.yale.edu/ligpargen/) [34, 35, 36]. The protein was solvated in a dodecahedron box using a three-point water model, and neutralized with sodium (Na+) and chloride (Cl-) ions as counterions. The protein-ligand system was then subjected to energy minimization using the 'gmx grompp' and 'gmx mdrun' commands. Equilibration was carried out under NVT (Canonical) and NPT (Isobaric) ensembles, with the V-rescale thermostat applied to maintain a constant volume and temperature of 300 K. The complex was subjected to MD simulation run for 100 ns. To assess the stability of the complex, various analyses were conducted using the 'gmx rms' command, including root mean square deviation (RMSD), root mean square fluctuation (RMSF), radius of gyration (Rg), solvent-accessible surface area (SASA) and hydrogen bond count (HBond).

3. Result and Discussion

3.1 Network Pharmacology

3.1.1 Target Prediction and Collection of T2DM Targets

From the literature, 16 active constituents of karela (Momordicilin, Momordicoside C, Momorcharaside B, Momordin I, Cucurbitacin, Cycloartanol, Momordicoside A, Momordicoside L, Momordenol, Karounidiol, Momordicoside K, Momordicoside B, Momordicin, Cucurbitane, Charine, and Cucurbitine) were shortlisted and their SMILES and 3D structures downloaded from the PubChem database **(Table:1).** Using BindingDB and SwissTargetPrediction, 776 potential targets of the 16 active constituents of Karela were identified. For the collection of T2DM targets, the Open Target (5119 targets), TTD (187 targets), and DisGeNet (2826 targets) databases were used. The UniProt ID for each target was provided, and from the three databases, a final set of 104 T2DM targets was selected for study. A Venn diagram revealed 49 overlapping targets of T2DM and Karela, as listed in **Table:2**, for further study.

3.1.2 Gene Ontology (GO) and Kyoto Encyclopedia of Genes and Genomes (KEGG) pathway enrichment

To explore the multiple functions of 49 targets, GO and KEGG analysis were performed. In GO analysis 279 biological process (BP), 34 cellular components (CC), and 46 molecular functions (MF) were enriched out of which top 10 BP, CC and MF have been represented in Fig. 1A. The targets of karela in treating T2DM were primarily enriched in the following categories (i) Biological Processes (BP): positive regulation of gene expression, protein phosphorylation, inflammatory response, and signal transduction (ii) Cellular Components (CC): plasma membrane, cytoplasm, cytosol, and integral components of the membrane and (iii) Molecular Functions (MF): protein binding, ATP binding, integral protein binding, and protein serine/threonine/tyrosine kinase activity. The 140 pathways were enriched in KEGG analysis where the top 2 were found to be type 2 diabetes mellitus and Insulin resistance. The top 10 enriched pathways are depicted in Fig. 1B.

3.1.3 Network Analysis

The intersection targets of T2DM and Karela are presented as Venn diagram in Fig. 2A. The PPI network of these 49 targets were generated using STRING database and analysed in cystoscope as depicted in Fig. 2B. This network comprised of 49 nodes and 44 edges with an average node degree of 1.8 and a low PPI enrichment P-value of 4.83e-13. The MCODE plugin in Cytoscape was utilized to identify clusters representing highly interconnected areas within a network. In present study, this analysis unveiled a highly interconnected region and PRKCD as hub gene as depicted in Fig. 2C. The Cytohubba plug in was used to identify top 10 genes from network, based on closeness and degree calculations, as shown in Fig. 2D and Fig. 2E. CytoNCA, which provides various centrality metrics for both, weighted and unweighted networks, was employed to analyse the selected network for closeness, betweenness, and degree calculations without applying weights. The identified top 10 highly interconnected genes are presented in **Table: 3.** Various studies have indicated that the overexpression of PRKCD leads to insulin resistance. Olivier B. et al. revealed in their study that in hepatic cells, the overexpression of PRKCD in C57BL/6J and 129S6/Sv mice resulted in glucose intolerance, insulin resistance and overexpression of gluconeogenic enzymes. PRKCD also plays a role in diabetic microvascular complications such as diabetic nephropathy, diabetic retinopathy, and diabetic neuropathy [37, 38, 39]. Based on these studies, it can be concluded that PRKCD plays a significant role in the pathology of T2DM, and this target has been selected for further molecular docking and MD simulation studies.

3.1.4 Differential Gene Expression Analysis

To prove further pathophysiological role of PRKCD in T2DM, we performed the gene expression analysis. The GSE26168 dataset (https://www.ncbi.nlm.nih.gov/geoprofiles/74421147) was downloaded from GEO database. This study includes 24 patients (8 control, 7 with impaired fasting glucose and 9 with T2DM) and PRKCD levels in their blood were analysed. As shown in Fig. 3, prediabetic patients with impaired fasting glucose exhibited significant overexpression of PRKCD in their blood compared to the control group and a similar overexpression of PRKCD was observed in T2DM patients. This indicates that identified gene PRKCD plays a crucial role in T2DM and inhibition of its expression may be an effective approach for treating T2DM.

3.2 Prediction of Binding Pocket

Predicted binding pockets of PRKCD protein through CastP and PocketDepth servers shown in **Table:4**. Amino acid involved in molecular docking interaction highlighted with yellow colour.

3.3 Molecular Docking

Molecular docking of the 16 active constituents of Karela with the PRKCD protein was performed, and the molecular docking scores along with interactions with various amino acids are shown in **Table:5**. The molecular docking score ranges from − 8.2 kcal/mol to -4.7 kcal/mol. The top scored compound, Momordicilin, did not shown any H-bonding with any amino acid. The top three compounds were Momordicoside C, Momorcharaside B and Momordin I with molecular docking score of -8.0 kcal/mol, -7.9 kcal/mol and − 7.9 kcal/mol respectively. Momordicoside C aglycone part formed H-bond with Ala23, Gln25, Arg75 with distance of 2.30 Å, 1.99 Å, 2.79 Å and 2.53 Å respectively. While Momorcharaside B aglycone group formed two H-bond with Pro26, Gln25 with distance of 2.46 Å and 2.30 Å respectively. Momordin I aglycone group formed H-bond with Ser5 with a distance of 2.26 Å and glycone part formed H-bond with Ile6, Gln8 (2 H-bond), Val11 (2 H-bond), Tyr52 and Thr58 with distance of 2.57 Å, 2.30 Å, 1.85 Å, 2.25 Å, 2.19 Å, 2.43 Å and 3.16 Å. The 2D and 3D interaction of top 3 compounds Momorcharaside B, Momordicoside C and Momordin I are presented in a Fig. 4A, Fig. 4B and Fig. 4C.

3.4 MD Simulation

The complex of PRKCD and ligand subjected to 100ns of MD simulation and the various parameters were measures like RMSD, RMSF, Rg and SASA. The RMSD is used for checking the stability of complex and lower RMSD value indicates the stable complex [40–43]. The RMSD of Momorcharaside B in Fig. 5A. After 20 ns of fluctuation, the complex of PRKCD and Momorcharaside B (grey) became stable, with an RMSD value of around 1 nm, indicating a stable complex. The RMSD value of the PRKCD protein(blue) alone was also lower, around 0.2 nm. RMSF analysis describes the fluctuations of amino acids throughout the 100 ns simulation. A higher RMSF value signifies greater amino acid movement during the simulation [37–40]. The Fig. 5B represents the RMSF of complex and its showed that there is less fluctuations and at the end of the simulation the RMSF value is around 0.7nm. For analysis of stability and folding properties of protein SASA was calculated [37–40]. The Fig. 5C represents the SASA of protein(blue), Lig (orange) and complex (grey). The SASA value of protein and complex is almost same and there is no instability during the 100ns of simulation. The Rg value indicates the compactness and stability of system. The Fig. 5D despites the Rg of Protein (blue), Lig (orange) and Complex(gray). After 20ns of fluctuations complex remain stable throughout the 100ns of simulation and after 70ns the protein and complex are overlapped and Rg value being less than 1.7nm and this indicates the stable system. Hydrogen bonding analysis is essential for characterizing ligand-protein interactions, as hydrogen bonds can influence the binding strength of small molecules [37–40]. As represented in Fig. 5E PRKCD and Momorcharaside B complex formed the 3 H-bond at the end of the simulation. Figure 5F represents the distance of donor- acceptor H-bond during the simulation.

Figure 6 presents the MD simulation data for Momordicoside C. Figure 6A showed the RMSD values of the system. Due to initial conformational changes in the protein during the first 25 ns, the RMSD value of the complex (grey) rose to 2 nm, but it stabilized, and by the end of the simulation, the RMSD value was close to 1 nm, indicating a stable and compact system. The RMSF value was observed to be around 1.4 nm (Fig. 6B), and the SASA (Fig. 6C) for both the complex (grey) and protein (blue) remained stable throughout the simulation. The Rg value of the complex (Fig. 6D) fluctuated during the simulation. Up until 50 ns, the complex remained stable, but at 50 ns, there was a fluctuation with the Rg value reaching up to 4 nm. It stabilized again, but another fluctuation occurred at 70 ns. By the end of the 100 ns simulation, the Rg value was near 2 nm. Figure 6E represents the number of hydrogen bonds formed during the simulation. From this MD analysis, It can conclude that the complex of Momordicoside C is quite stable.

Figure 7A showed the RMSD of Momordin I. As depicted, the complex remained stable between 20 to 70 ns, but fluctuations began afterward, with the RMSD rising to 3.5 nm. However, there was minimal fluctuation in the RMSF (Fig. 7B) and SASA (Fig. 7C), with the RMSF remaining close to 0.8 nm. The Rg of the complex (Fig. 7D) was near 3.5 nm at the end of the simulation, although there was some instability throughout the process. By the end of the simulation, no hydrogen bond

interactions were observed (Fig. 7E), suggesting that the Momordin I complex is not stable. Figure 8 showed the amino acid interactions of all three compounds at 0 ns (Fig. 8A), 50 ns (Fig. 8B), and 100 ns (Fig. 8C). By the end of the simulation, Momorcharaside B formed three hydrogen bonds, Momordicoside C formed four hydrogen bonds, and Momordin I did not form any hydrogen bonds with the PRKCD protein. Therefore, Momorcharaside B and Momordicoside C could act as potential PRKCD inhibitors for the treatment of T2DM.

4. Summary

Type 2 diabetes mellitus being the most prevalent disorder, linked to insulin resistance and insufficient insulin production. Natural products, including Momordica charantia (bitter melon or karela), are increasingly explored for their anti-diabetic properties due to fewer side effects and affordability. Bitter melon contains several bioactive compounds like saponins and alkaloids, known for their hypoglycemic activity. This study aimed to explore additional anti-diabetic mechanisms of karela through network pharmacology, molecular docking, and MD simulation.

Network pharmacology identified 49 overlapping targets between T2DM and karela, highlighting PRKCD as a key target. Gene expression analysis confirmed the overexpression of PRKCD in prediabetic and diabetic patients. PRKCD belongs to the family of serine/threonine protein kinases [44], and this was further confirmed by the GO enrichment study, where it was identified as a molecular function (Fig. 1A). Figure 1C illustrates the KEGG enrichment of PRKCD, and as shown in the figure, hyperglycemia triggers the activation of PRKCD, leading to insulin resistance. The PRKCD is also involved in various cellular process for developing T2DM [45]. Activation of this protein can increase the glucose level, this hyperglycemia condition can trigger the glycolysis pathway and increased synthesis of diacylglycerol (DAG) which ultimately leads activation protein kinase and this promotes the oxidative stress in body and as consequence of this it leads to cell death and apoptosis. [46, 47]. So, deactivation of PRKCD can be beneficial for the tratemnet of T2DM. Molecular docking of 16 karela compounds with PRKCD revealed top-binding compounds: Momordicoside C, Momorcharaside B, and Momordin I. MD simulations demonstrated stable interactions between PRKCD and Momorcharaside B, suggesting potential as a PRKCD inhibitor, which could be beneficial for T2DM management. Figure 9 represents the proposed mechanism of Momorcharaside B, Momordicoside C in the treatment of T2DM. Deactivation of PRKCD can lead regulation of MAPK pathway and less/no generation of reactive oxygen species and no insulin resistance.

5. Conclusion

In conclusion, this study highlights the therapeutic potential of Momordica charantia (bitter melon) as a natural remedy for T2DM. Through network pharmacology analysis, 49 target proteins were identified that link the active constituents of Momordica charantia to T2DM. Among these targets, PRKCD emerged as a key hub gene and it is associated with insulin resistance and diabetic complications. Molecular docking studies revealed that the active compounds Momorcharaside B, Momordicoside C, and Momordin I interact with PRKCD. Momorcharaside B and Momordicoside C demonstrating the most stable interactions during 100ns of molecular dynamics simulations. These findings suggest that these two compounds have the potential to act as PRKCD inhibitors, offering a novel mechanism for managing T2DM. The results provide a foundation for further research and development of Momordica charantia-derived treatments, emphasizing the role of natural products in combating chronic metabolic diseases like diabetes.

Declarations

Conflict of Interest Statement: Declared None

CRediT Statement:

Yadav Ruchi: Data Curation, Writing - Original Draft, Visualization; **Nidhi Nambir** and **Manushi Shah**: Collection of the data from various sources and databases; **Patel Bhumika:** Conceptualization, Methodology, Supervision, Writing - Review &

Editing, English editing

Acknowledgment: Authors are thankful to Nirma University, Ahmedabad, Gujarat, India for providing necessary facilities to carry out this research work.

References

1. Ogurtsova, K., da Rocha Fernandes, J. D., Huang, Y., Linnenkamp, U., Guariguata, L., Cho, N. H., ... & Makaroff, L. E. (2017). IDF Diabetes Atlas: Global estimates for the prevalence of diabetes for 2015 and 2040. *Diabetes research and clinical practice*, 128, 40-50. https://doi.org/10.1016/j.diabres.2017.03.024
2. Tsalamandris S, Antonopoulos AS et. al, The role of inflammation in diabetes: current concepts and future perspectives. *Eur Cardiol.* **2019**, 14(1):50. https://doi.org/10.15420/ecr.2018.33.1
3. Safiri, S., Karamzad, N., Kaufman, J. S., Bell, A. W., Nejadghaderi, S. A., Sullman, M. J., ... & Kolahi, A. A. (2022). Prevalence, deaths and disability-adjusted-life-years (DALYs) due to type 2 diabetes and its attributable risk factors in 204 countries and territories, 1990-2019: results from the global burden of disease study 2019. *Frontiers in endocrinology*, 13, 838027. https://doi.org/10.3389/fendo.2022.838027
4. Himanshu, D., Ali, W., & Wamique, M. (2020). Type 2 diabetes mellitus: pathogenesis and genetic diagnosis. *Journal of Diabetes & Metabolic Disorders*, 19, 1959-1966. . https://doi.org/10.1007/s40200-020-00641-x
5. Galicia-Garcia, U., Benito-Vicente, A., Jebari, S., Larrea-Sebal, A., Siddiqi, H., Uribe, K. B., ... & Martín, C. (2020). Pathophysiology of type 2 diabetes mellitus. *International journal of molecular sciences*, 21(17), 6275. https://doi.org/10.3390/ijms21176275
6. Choudhury, H., Pandey, M., Hua, C. K., Mun, C. S., Jing, J. K., Kong, L., ... & Kesharwani, P. (2018). An update on natural compounds in the remedy of diabetes mellitus: A systematic review. *Journal of traditional and complementary medicine*, 8(3), 361-376.https://doi.org/10.1016/j.jtcme.2017.08.012
7. Jain PK, Das D et. al, Traditional Indian herb Emblica officinalis and its medicinal importance. *International Journal of Pharmacy and Pharmaceutical Sciences*. **2016**, 4(4):1-5.
8. Pandit, S., Kanjilal, S., Awasthi, A., Chaudhary, A., Banerjee, D., Bhatt, B. N., ... & Katiyar, C. K. (2017). Evaluation of herb-drug interaction of a polyherbal Ayurvedic formulation through high throughput cytochrome P450 enzyme inhibition assay. *Journal of ethnopharmacology*, 197, 165-172. https://doi.org/10.1016/j.jep.2016.07.061
9. Richter, E., Geetha, T., Burnett, D., Broderick, T. L., & Babu, J. R. (2023). The effects of Momordica charantia on type 2 diabetes mellitus and Alzheimer's disease. *International Journal of Molecular Sciences*, 24(5), 4643. https://doi.org/10.3390/ijms24054643
10. Joseph, B., & Jini, D. (2013). Antidiabetic effects of Momordica charantia (bitter melon) and its medicinal potency. *Asian pacific journal of tropical disease*, 3(2), 93-102. https://doi.org/10.1016/S2222-1808(13)60052-3
11. Mahmoud, M. F., Hassan, N. A., El Bassossy, H. M., & Fahmy, A. (2013). Quercetin protects against diabetes-induced exaggerated vasoconstriction in rats: effect on low grade inflammation. *PloS one*, 8(5), e63784. https://doi.org/10.1371/journal.pone.0063784
12. Matsuda, H., Li, Y., Murakami, T., Matsumura, N., Yamahara, J., & Yoshikawa, M. (1998). Antidiabetic principles of natural medicines. III. Structure-related inhibitory activity and action mode of oleanolic acid glycosides on hypoglycemic activity. *Chemical and Pharmaceutical Bulletin*, 46(9), 1399-1403. https://doi.org/10.1248/cpb.46.1399
13. Raman, A., & Lau, C. (1996). Anti-diabetic properties and phytochemistry of Momordica charantia L.(Cucurbitaceae). *Phytomedicine*, 2(4), 349-362. https://doi.org/10.1016/S0944-7113(96)80080-8
14. Liu, T., Lin, Y., Wen, X., Jorissen, R. N., & Gilson, M. K. (2007). BindingDB: a web-accessible database of experimentally determined protein–ligand binding affinities. *Nucleic acids research*, 35(suppl_1), D198-D201.
15. Daina, A., Michielin, O., & Zoete, V. (2019). SwissTargetPrediction: updated data and new features for efficient prediction of protein targets of small molecules. *Nucleic acids research*, 47(W1), W357-W364.

https://doi.org/10.1093/nar/gkz382

16. Piñero J, Ramírez-Anguita JM, Saüch-Pitarch J, Ronzano F, Centeno E, Sanz F, Furlong LI. (2020) The DisGeNET knowledge platform for disease genomics: 2019 update. *Nucleic acids research,* 48(D1):D845-D855. https://doi.org/10.1093/nar/gkz1021
17. Zhou, Y., Zhang, Y., Zhao, D., Yu, X., Shen, X., Zhou, Y., ... & Zhu, F. (2024). TTD: Therapeutic Target Database describing target druggability information. *Nucleic acids research,* 52(D1), D1465-D1477. https://doi.org/10.1093/nar/gkad751
18. Ochoa, D., Hercules, A., Carmona, M., Suveges, D., Baker, J., Malangone, C., ... & McDonagh, E. M. (2023). The next-generation Open Targets Platform: reimagined, redesigned, rebuilt. *Nucleic acids research*, 51(D1), D1353-D1359. https://doi.org/10.1093/nar/gkac1046
19. Coudert, E., Gehant, S., De Castro, E., Pozzato, M., Baratin, D., Neto, T., ... & Bridge, A. (2023). Annotation of biologically relevant ligands in UniProtKB using ChEBI. *Bioinformatics,* 39(1), btac793. https://doi.org/10.1093/bioinformatics/btac793
20. JC Oliveros. VENNY. An interactive tool for comparing lists with Venn Diagrams. http://bioinfogp. cnb. csic. es/tools/venny/index. html. 2007.
21. Szklarczyk, D., Kirsch, R., Koutrouli, M., Nastou, K., Mehryary, F., Hachilif, R., ... & Von Mering, C. (2023). The STRING database in 2023: protein–protein association networks and functional enrichment analyses for any sequenced genome of interest. *Nucleic acids research*, 51(D1), D638-D646. https://doi.org/10.1093/nar/gkac1000
22. Shannon, P., Markiel, A., Ozier, O., Baliga, N. S., Wang, J. T., Ramage, D., ... & Ideker, T. (2003). Cytoscape: a software environment for integrated models of biomolecular interaction networks. *Genome research*, 13(11), 2498-2504. http://www.genome.org/cgi/doi/10.1101/gr.1239303.
23. ader, G. D., & Hogue, C. W. (2003). An automated method for finding molecular complexes in large protein interaction networks. *BMC bioinformatics*, 4, 1-27. https://doi.org/10.1186/1471-2105-4-2
24. Chin, C. H., Chen, S. H., Wu, H. H., Ho, C. W., Ko, M. T., & Lin, C. Y. (2014). cytoHubba: identifying hub objects and sub-networks from complex interactome. *BMC systems biology*, 8, 1-7. https://doi.org/10.1186/1752-0509-8-S4-S11
25. Tang, Y., Li, M., Wang, J., Pan, Y., Wu, F.X.(2015) CytoNCA: a cytoscape plugin for centrality analysis and evaluation of protein interaction networks. *Biosystems*, 127:67-72. https://doi.org/10.1016/j.biosystems.2014.11.005
26. Sherman, B. T., Hao, M., Qiu, J., Jiao, X., Baseler, M. W., Lane, H. C., ... & Chang, W. (2022). DAVID: a web server for functional enrichment analysis and functional annotation of gene lists (2021 update). *Nucleic acids research*, 50(W1), W216-W221. https://doi.org/10.1093/nar/gkac194
27. Kanehisa, M., Furumichi, M., Sato, Y., Kawashima, M., & Ishiguro-Watanabe, M. (2023). KEGG for taxonomy-based analysis of pathways and genomes. *Nucleic acids research*, 51(D1), D587-D592. https://doi.org/10.1093/nar/gkac963
28. Tang, D., Chen, M., Huang, X., Zhang, G., Zeng, L., Zhang, G., ... & Wang, Y. (2023). SRplot: A free online platform for data visualization and graphing. *PLoS One*, 18(11), e0294236. https://doi.org/10.1371/journal.pone.0294236
29. Kalidas Y, Chandra N. PocketDepth: a new depth based algorithm for identification of ligand binding sites in proteins (2008). *J Struct Biol.* 2008, 161(1):31-42. https://doi.org/10.1016/j.jsb.2007.09.005.
30. Bowei Ye, Wei Tian, Boshen Wang, Jie Liang, CASTpFold: Computed Atlas of Surface Topography of the universe of protein Folds(2024). *Nuc. Acids Res.*, 52(W1):W194–W199, https://doi.org/10.1093/nar/gkae415.
31. Meng, X. Y., Zhang, H. X., Mezei, M., & Cui, M. (2011). Molecular docking: a powerful approach for structure-based drug discovery. *Current computer-aided drug design*, 7(2), 146-157. https://doi.org/10.2174/157340911795677602
32. Eberhardt, J., Santos-Martins, D., Tillack, A. F., & Forli, S. (2021). AutoDock Vina 1.2. 0: New docking methods, expanded force field, and python bindings. *Journal of chemical information and modeling*, 61(8), 3891-3898. https://doi.org/10.1021/acs.jcim.1c00203
33. Bekker, H., Berendsen, H. J. C., Dijkstra, E. J., Achterop, S., Vondrumen, R. V., Vanderspoel, D., ... & Renardus, M. K. R. (1993). Gromacs-a parallel computer for molecular-dynamics simulations. In 4th international conference on

computational physics (PC 92) (pp. 252-256). World Scientific Publishing.

34. Jorgensen, W. L., & Tirado-Rives, J. (2005). Potential energy functions for atomic-level simulations of water and organic and biomolecular systems. *Proceedings of the National Academy of Sciences*, 102(19), 6665-6670. https://doi.org/10.1073/pnas.0408037102
35. Dodda, L. S., Vilseck, J. Z., Tirado-Rives, J., & Jorgensen, W. L. (2017). 1.14* CM1A-LBCC: localized bond-charge corrected CM1A charges for condensed-phase simulations. *The Journal of Physical Chemistry*, 121(15), 3864-3870. https://doi.org/10.1021/acs.jpcb.7b00272
36. Dodda, L. S., Cabeza de Vaca, I., Tirado-Rives, J., & Jorgensen, W. L. (2017). LigParGen web server: an automatic OPLS-AA parameter generator for organic ligands. Nucleic acids research, 45(W1), W331-W336. https://doi.org/10.1093/nar/gkx312
37. Bezy, O., Tran, T. T., Pihlajamäki, J., Suzuki, R., Emanuelli, B., Winnay, J., ... & Kahn, C. R. (2011). PKCδ regulates hepatic insulin sensitivity and hepatosteatosis in mice and humans. *The Journal of clinical investigation*, 121(6), 2504-2517. https://doi.org/10.1172/JCI46045
38. Pan, D., Xu, L., & Guo, M. (2022). The role of protein kinase C in diabetic microvascular complications. *Frontiers in Endocrinology*, 13, 973058. https://doi.org/10.3389/fendo.2022.973058
39. Geraldes, P., & King, G. L. (2010). Activation of protein kinase C isoforms and its impact on diabetic complications. *Circulation research*, 106(8), 1319-1331. https://doi.org/10.1161/CIRCRESAHA.110.217117.
40. Yu M, Shen Z, Zhang S, Zhang Y, Zhao H, Zhang L. (2024) The active components of Erzhi wan and their anti-Alzheimer's disease mechanisms determined by an integrative approach of network pharmacology, bioinformatics, molecular docking, and molecular dynamics simulation. *Heliyon*. 202410(13):e33761. https://doi.org/10.1016/j.heliyon.2024.e33761.
41. Mao T, Chen B, Wei W, Chen G, Liu Z, Wu L, Li X, Pathak JL, Li J. (2024) AutoDock and molecular dynamics-based therapeutic potential prediction of flavonoids for primary Sjögren's syndrome. *Heliyon,* 10(13):e33860. https://doi.org/10.1016/j.heliyon.2024.e33860.
42. Yang, P., Liu, P., & Li, J. (2022). The regulatory network of gastric cancer pathogenesis and its potential therapeutic active ingredients of traditional Chinese medicine based on bioinformatics, molecular docking, and molecular dynamics simulation*. Evidence-Based Complementary and Alternative Medicine,* 2022(1), 5005498. https://doi.org/10.1155/2022/5005498.
43. Tang, L., Liu, Y., Tao, H., Feng, W., & Ren, C. (2024). Network pharmacology integrated with molecular docking and molecular dynamics simulations to explore the mechanism of Tongxie Yaofang in the treatment of ulcerative colitis. *Medicine*, 103(36), e39569. https://doi.org/10.1097/MD.0000000000039569.
44. Mochly-Rosen, D., Das, K., & Grimes, K. V. (2012). Protein kinase C, an elusive therapeutic target?. *Nature reviews Drug discovery*, 11(12), 937-957. https://doi.org/10.1038/nrd3871
45. Xia, P., Inoguchi, T., Kern, T. S., Engerman, R. L., Oates, P. J., & King, G. L. (1994). Characterization of the mechanism for the chronic activation of diacylglycerol-protein kinase C pathway in diabetes and hypergalactosemia. *Diabetes*, 43(9), 1122-1129. https://doi.org/10.2337/diab.43.9.1122
46. Wang QJ. PKD at the crossroads of DAG and PKC signaling. Trends Pharmacol Sci (2006) 27(6):317–23. doi: 10.1016/j.tips.2006.04.003
47. Jang JH, Kim EA, Park HJ, Sung EG, Song IH, Kim JY, et al. Methylglyoxal-induced apoptosis is dependent on the suppression of c-FLIP(L) expression via down-regulation of p65 in endothelial cells. J Cell Mol Med (2017) 21(11):2720–31. doi: 10.1111/jcmm.13188

Tables

Table 1 is available in the Supplementary Files section.

Table 2. Possible overlap between 49 targets of T2DM and Karela

Sr. No	Uniprot ID	Gene Name	Sr. No	Uniprot ID	Gene Name
1	O00763	ACACB	26	MAPK1	P28482
2	P30542	ADORA1	27	MAPK3	P27361
3	P29275	ADORA2B	28	MAPK8	P45983
4	P13945	ADRB3	29	MAPK9	P45984
5	P29466	CASP1	30	METAP2	P50579
6	Q14790	CASP8	31	MGAM	O43451
7	P32239	CCKBR	32	MTOR	P42345
8	P32246	CCR1	33	NOD2	Q9HC29
9	P51681	CCR5	34	NR3C1	P04150
10	P00746	CFD	35	P2RX7	Q99572
11	P21554	CNR1	36	PIK3CA	P42336
12	O75907	DGAT1	37	PIK3CB	P42338
13	P00734	F2	38	PIK3CD	O00329
14	P11362	FGFR1	39	PIK3CG	P48736
15	P47871	GCGR	40	PPARA	Q07869
16	Q8TDU6	GPBAR1	41	PPARD	Q03181
17	Q8TDV5	GPR119	42	PRKCD	Q05655
18	P49841	GSK3B	43	PRKCE	Q02156
19	P52789	HK2	44	REN	P00797
20	P28845	HSD11B1	45	SCD	O00767
21	P80365	HSD11B2	46	SIRT1	Q96EB6
22	P28223	HTR2A	47	SLC10A2	Q12908
23	O14920	IKBKB	48	TLR9	Q9NR96
24	P01584	IL1B	49	TNF	P01375
25	P06213	INSR			

Table 3. Top 10 highly interconnected genes based on closeness, betweenness, and degree using CytoNCA

Sr. No	Closeness		Betweenness		Degree	
	Gene Name	Score	Gene Name	Score	Gene Name	Score
1	PRKCD	0.12676056	PRKCD	256.0	PRKCD	8.0
2	MAPK3	0.123853214	MAPK3	196.0	PIK3CB	7.0
3	PIK3CB	0.12328767	TNF	190.0	PIK3CD	7.0
4	PIK3CD	0.12328767	MTOR	76.0	PIK3CA	7.0
5	PIK3CA	0.12328767	PIK3CB	56.333332	TNF	5.0
6	MAPK1	0.12	PIK3CD	56.333332	MTOR	4.0
7	TNF	0.119469024	PIK3CA	56.333332	PRKCE	4.0
8	PRKCE	0.11790393	SIRT1	40.0	INSR	4.0
9	MAPK9	0.1173913	IL1B	37.0	IL1B	4.0
10	MAPK8	0.1173913	CASP1	37.0	1CASP1	4.0

Table: 4 Predicated Binding Pockets of PRKCD

CastP Server								PocketDepth Server			
Sr. No	Chain	Residue No	AminoAcid	Sr. No	Chain	Residue No	AminoAcid	Sr. No	Chain	Residue No	AminoAcid
1	A	-2	Gly	40	A	63	Ile	1	A	14	Leu
2	A	0	His	41	A	64	Tyr	2	A	16	Ser
3	A	1	Met	42	A	65	Glu	3	A	17	Leu
4	A	2	Ala	43	A	66	Gly	4	A	18	Gln
5	A	3	Pro	44	A	67	Arg	5	A	19	Ala
6	A	4	Phe	45	A	69	Ile	6	A	22	Glu
7	A	5	Leu	46	A	74	Met	7	A	23	Ala
8	A	6	Arg	47	A	75	Arg	8	A	24	Asn
9	A	7	Ile	48	A	89	Ser	9	A	25	Gln
10	A	8	Ala	49	A	77	Ala	10	A	26	Pro
11	A	9	Phe	50	A	88	Val	11	A	27	Phe
12	A	14	Leu	51	A	89	Ser	12	A	28	Cys
13	A	18	Gln	52	A	91	Leu	13	A	50	Thr
14	A	24	Asn	53	A	94	Arg	14	A	51	Met
15	A	26	Pro	54	A	95	Cys	15	A	52	Tyr
16	A	27	Phe	55	A	96	Lys	16	A	53	Pro
17	A	28	Cys	56	A	99	Asn	17	A	54	Glu
18	A	30	Val	57	A	100	Gly	18	A	55	Trp
19	A	32	Met	58	A	101	Lys	19	A	57	Ser
20	A	33	Lys	59	A	102	Ala	20	A	58	Thr
21	A	34	Glu	60	A	104	Phe	21	A	59	Phe
22	A	40	Arg	61	A	117	Ser	22	A	60	Asp
23	A	41	Gly	62	A	118	Val	23	A	75	Arg
24	A	43	Thr	63	A	119	Gln	24	A	76	Ala
25	A	47	Lys	64	A	120	Tyr	25	A	77	Ala
26	A	48	Lys	65	A	121	Phe	26	A	79	Glu
27	A	49	Pro	66	A	122	Leu	27	B	8	Gln
28	A	50	Thr	67	A	123	Glu	28	B	10	Tyr
29	A	51	Met	68	B	2	Ala	29	B	11	Val
30	A	52	Tyr	69	B	3	Leu	30	B	12	Phe
31	A	53	Pro	70	B	4	Tyr	31	B	13	Ala
32	A	54	Glu	71	B	6	Ile				

33	A	55	Trp	72	B	8	Gln
34	A	57	Ser	73	B	9	Pro
35	A	58	Thr	74	B	10	Tyr
36	A	59	Phe	75	B	11	Val
37	A	60	Asp	76	B	12	Phe
38	A	61	Ala	77	B	13	Ala
39	A	62	His				

Table 5. Molecular docking interaction of active constituents of Karela

Sr. no	Compound Name	Molecular Docking Score (kcal/mol)	Amino acid interaction (H-bond)	Amino acid interaction (Hydrophobic)
1	Momordicilin	-8.2	NA	Tyr10, Phe12, Phe27, Tyr52
2	Momordicoside C	-8.0	Glycone: Tyr10 Aglycone: Ala23, Gln25, Arg75	Glycone: Tyr52, Aglycone: Phe27, Ala76
3	Momorcharaside B	-7.9	Aglycone: PRO26, GLN25	Glycone: Ala13, Ala23, Phe27, Tyr52
4	Momordin I	-7.9	Aglycone: Ser5, Ile6 Glycone: Gln8, Val11, Tyr52, Thr58	Glycone: Thr58
5	Cucurbitacin	-7.7	NA	Ala13, Tyr52
6	Cycloartanol	-7.6	NA	Tyr10, Phe12, Ala13, Phe27, Tyr52
7	Momordicoside A	-7.4	Glycone: Tyr10, Val11 Aglycone: Gln25, Glu54	Aglycone: Phe27, Trp55, Ala77
8	Momordicoside L	-7.4	Aglycone: Phe27, Tyr52, Trp55	Glycone: Tyr52
9	Momordenol	-7.2	NA	Phe27, Tyr52, Ala77, Met74
10	Karounidiol	-7.1	NA	Ala13, Phe27, Tyr52
11	Momordicoside K	-7.1	Glycone: Tyr10, Val11	Aglycone: Phe27, Trp55
12	Momordicoside B	-7.1	Glycone: Ala23, Gln25, Pro53	Aglycone: Tyr10, Val11, Ala13, Tyr52
13	Momordicin	-7.0	NA	Ala23, Gln25, Phe27
14	Cucurbitane	-6.9	NA	Ala13, Phe27, Tyr52
15	Charine	-5.7	Asp60, His62, Arg67	Lys48
16	Cucurbitine	-4.7	NA	Gln8, Asp60, His62

Figures

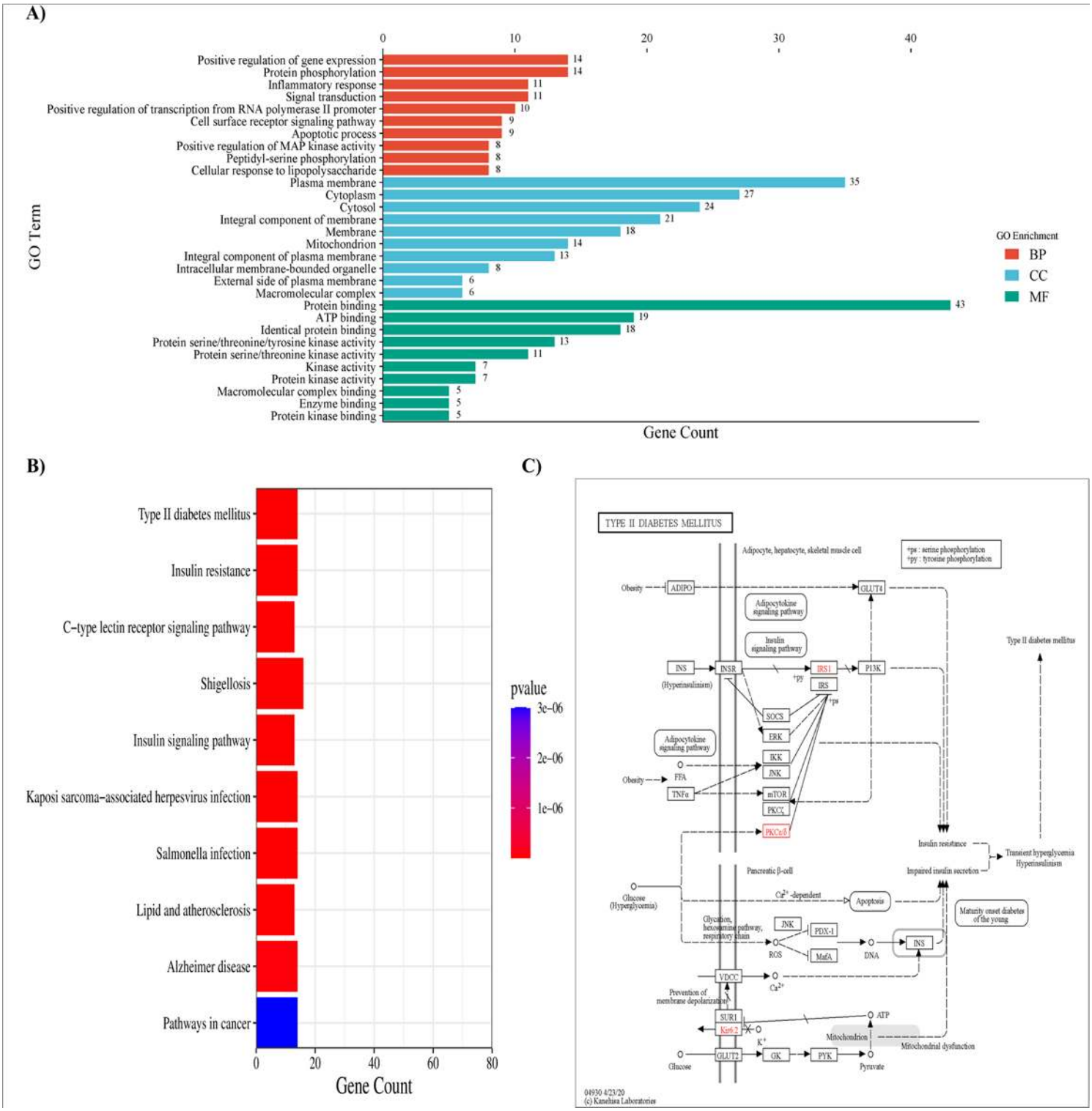


Figure 1

Enrichment analysis **A)** GO enrichment analysis of biological process (BP), cellular component (CC) and molecular function (MF). The size of the bars is arranged in the descending order of the number of genes **B)** KEGG pathway analysis of the top 10 targets. The bar color is displayed in a gradient from red to blue in ascending order of the p-value **C)** KEGG Enrichment of PRKCD

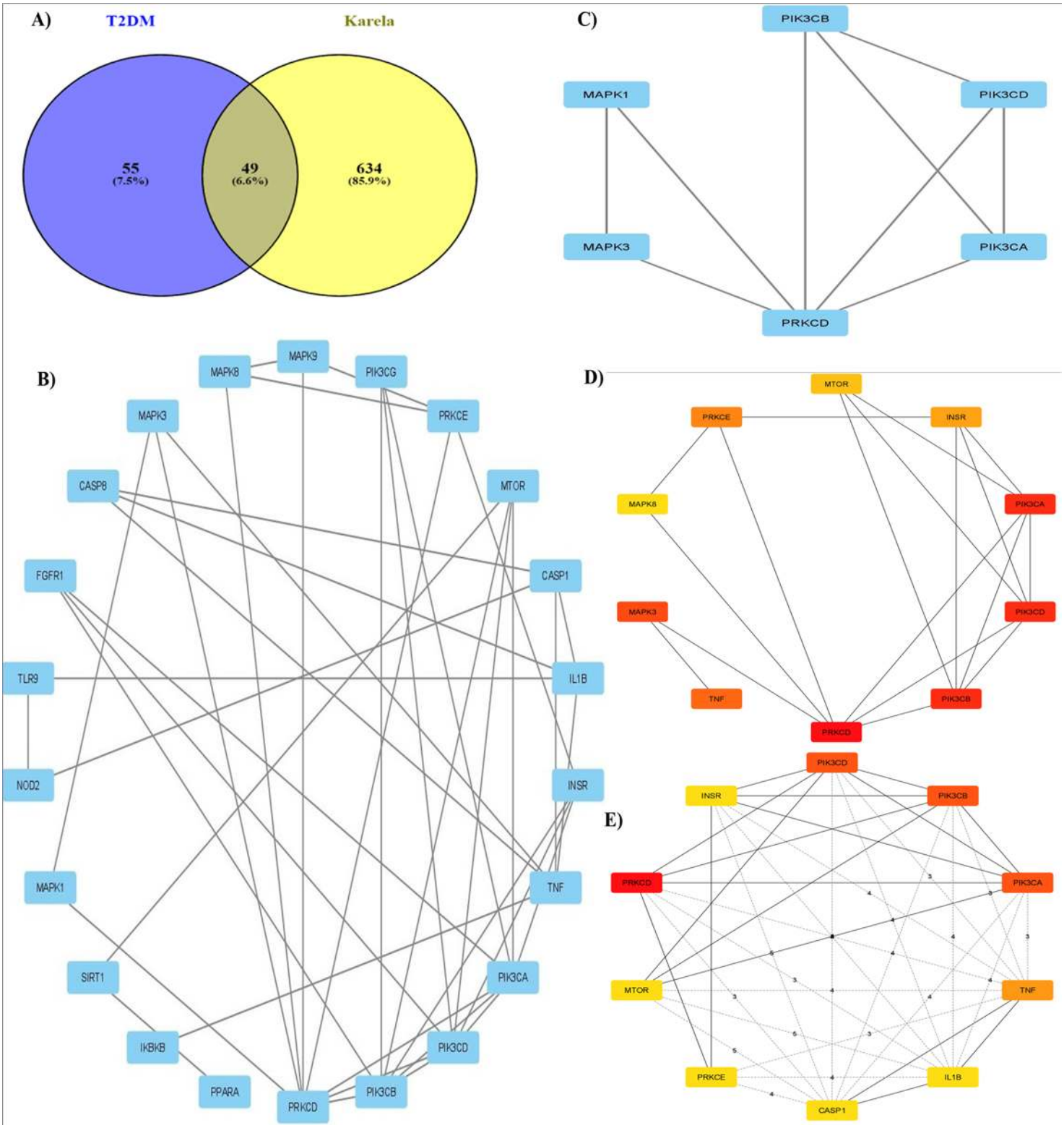


Figure 2

A) Venn diagram of targets of karela and T2DM **B)** Network of 49 targets **C)** Cluster 1 analysed by MCODE **D)** Top 10 genes based on closeness. Shades of red from dark to light indicates the genes from top to bottom in the list **E)** Top 10 genes based on degree. Shades of color: dark red indicates 1 number gene

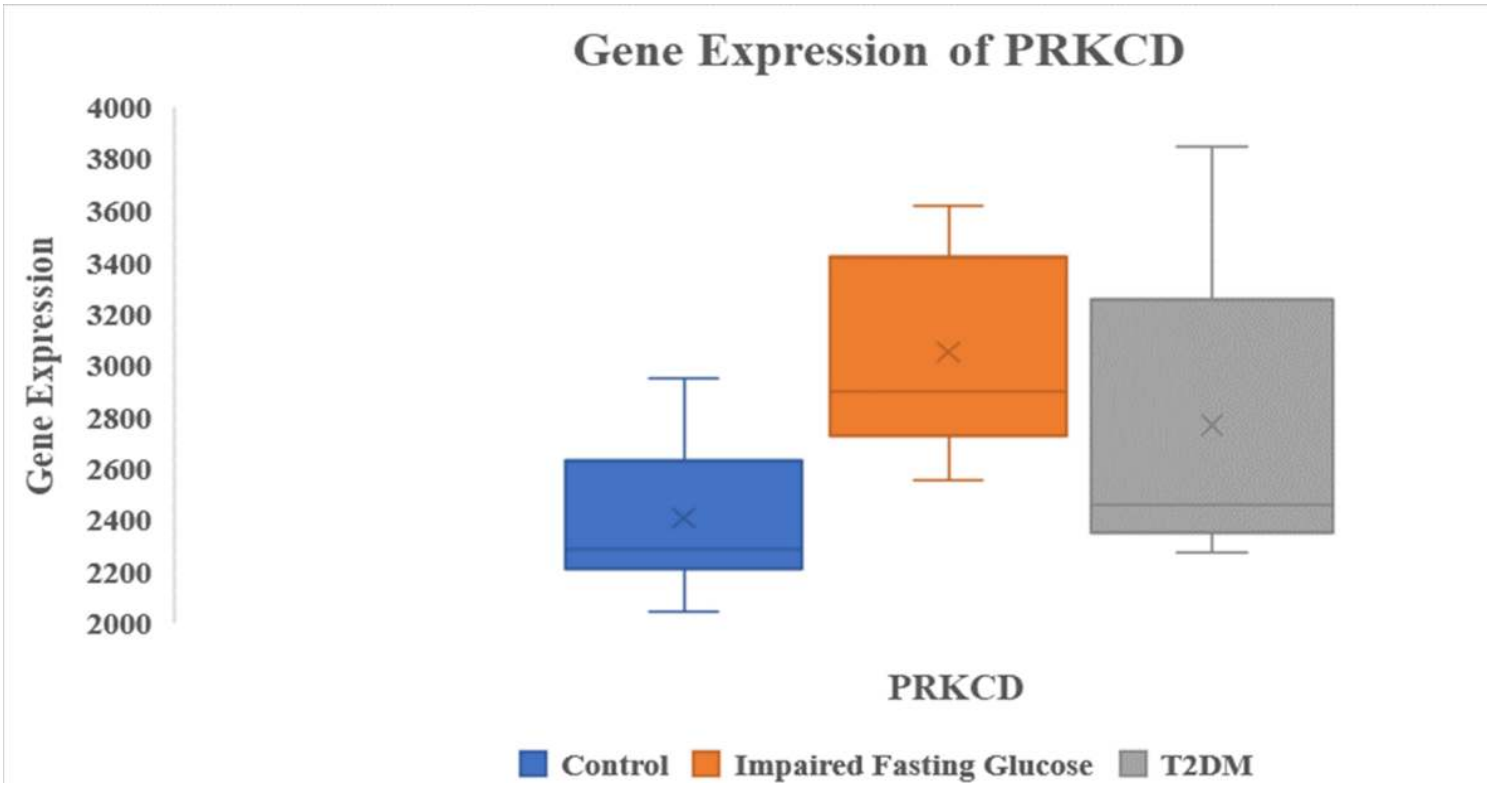


Figure 3

Gene expression of PRKCD in patient study

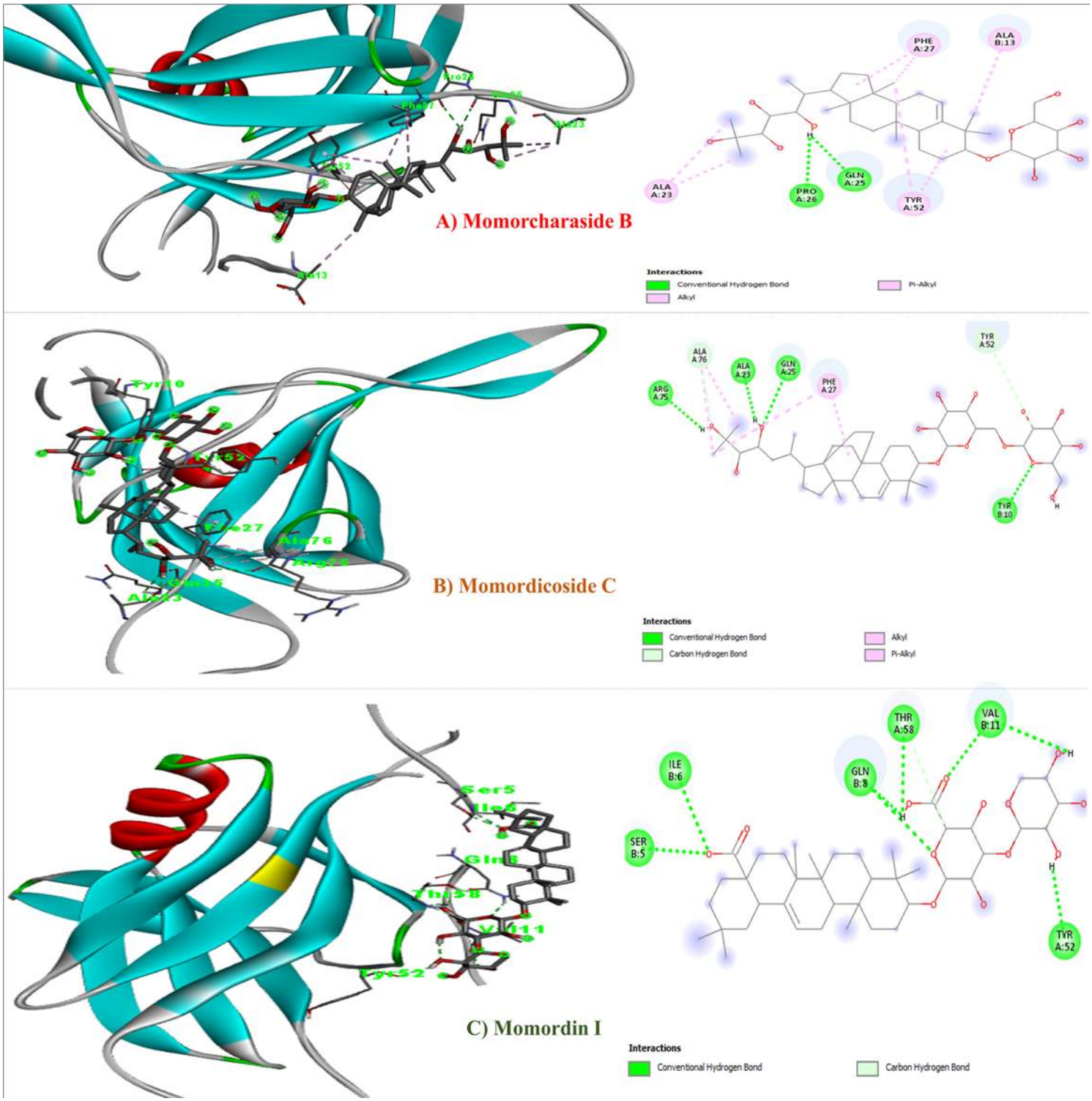


Figure 4

Molecular docking result **A)** 2D and 3D amino acid interaction of Momorcharaside B **B)** 2D and 3D amino acid interaction of Momordicoside C **C)** 2D and 3D amino acid interaction of Momordin I

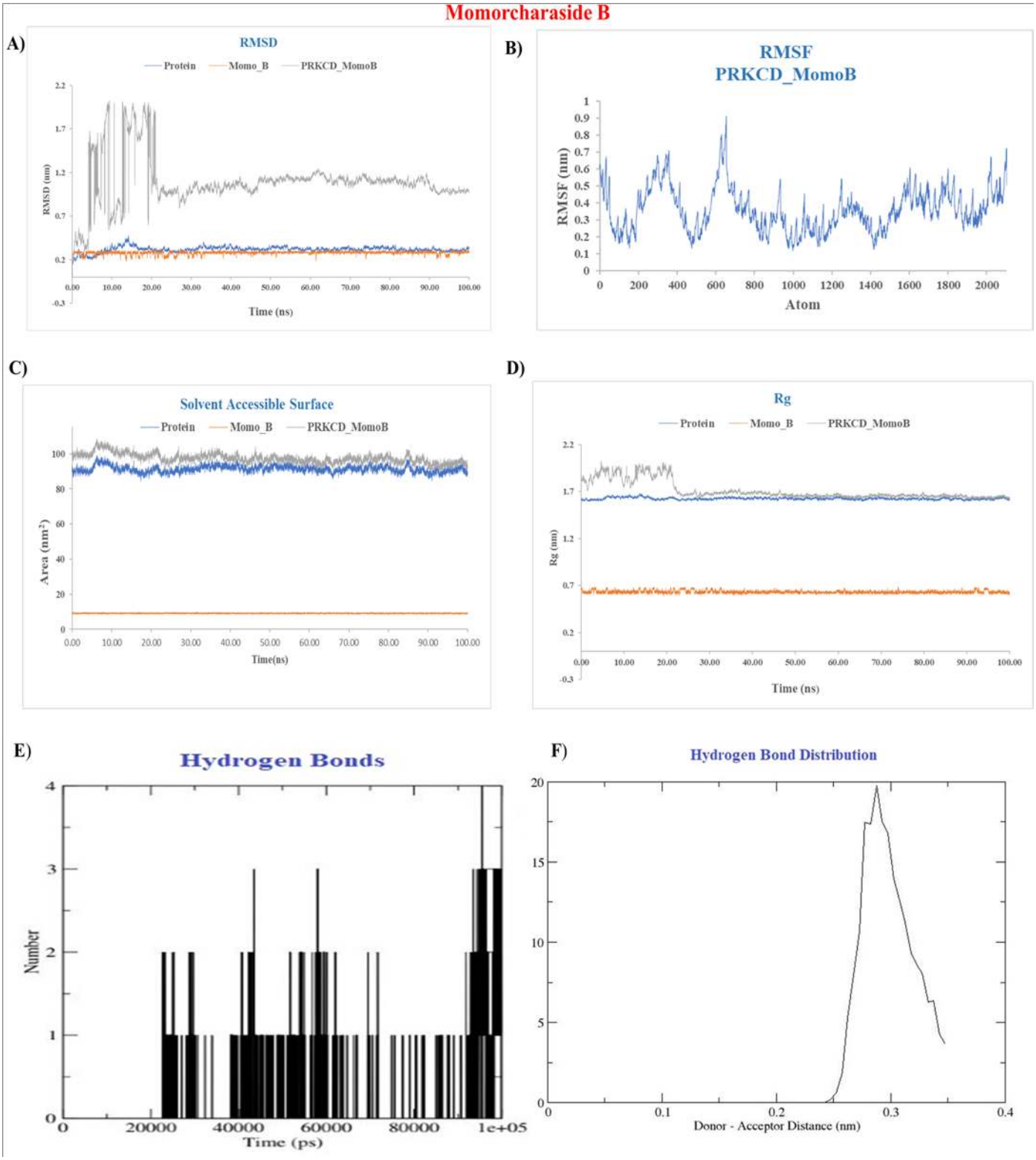


Figure 5

PRKCD interactions with the Momorcharaside B monitored during the 100 ns of simulation **A)**RMSD value (Protein: Blue, Momorcharaside B: Orange, Complex: Grey), **B)** RMSF of Complex **C)** SASA value (Protein: Blue, Momorcharaside B: Orange, Complex:Grey) **D)** Rg (Protein: Blue, Momorcharaside B: Orange, Complex: Grey) **E)** Number of H-bond **F)** Hydrogen bond distribution

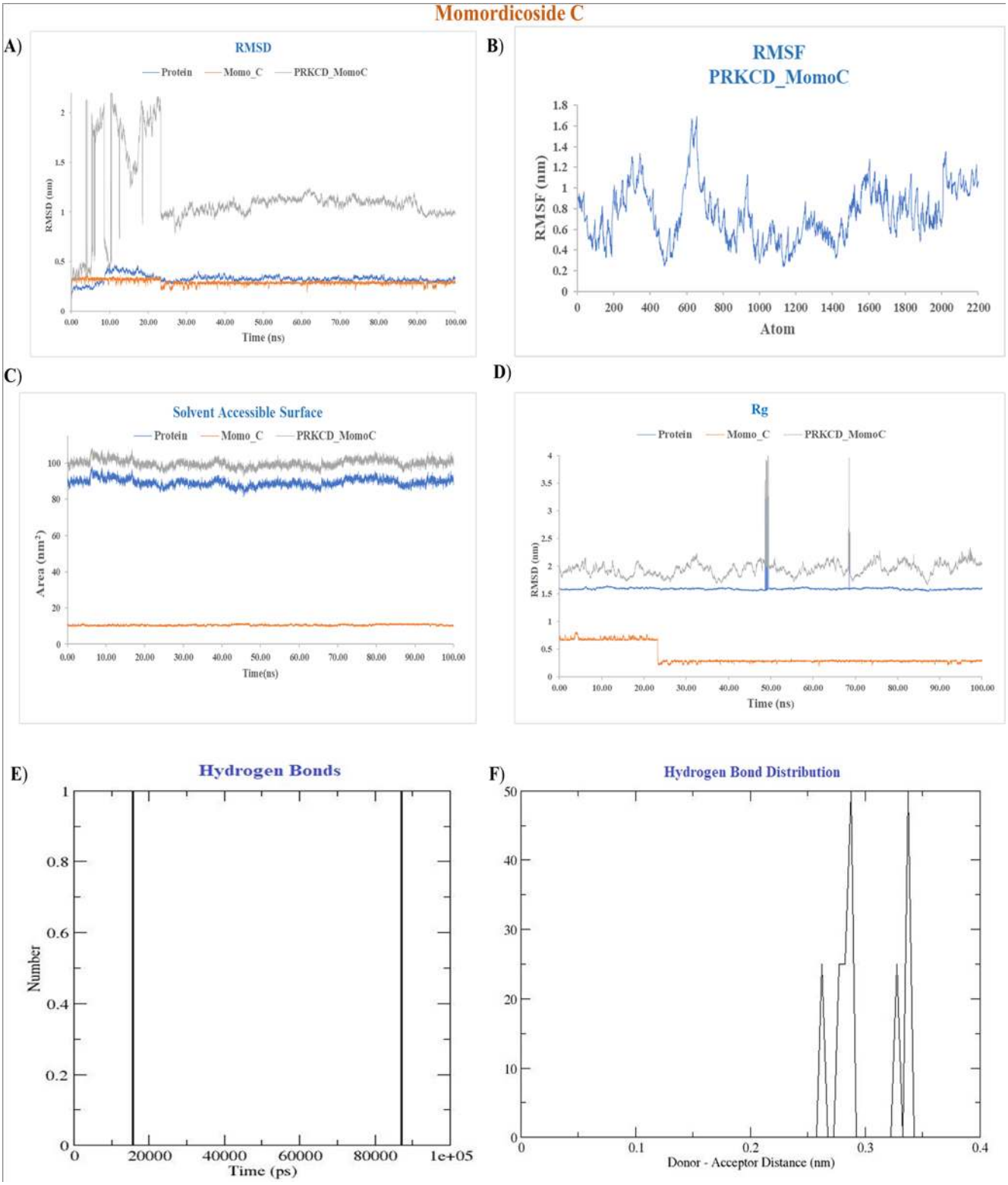


Figure 6

PRKCD interactions with the Momordicoside C monitored during the 100 ns of simulation **A)** RMSD value (Protein: Blue, Momordicoside C: Orange, Complex: Grey), **B)** RMSF of Complex **C)** SASA value (Protein: Blue, Momordicoside C: Orange, Complex: Grey) **D)** Rg (Protein: Blue, Momordicoside C: Orange, Complex: Grey) **E)** Number of H-bond **F)** Hydrogen bond distribution

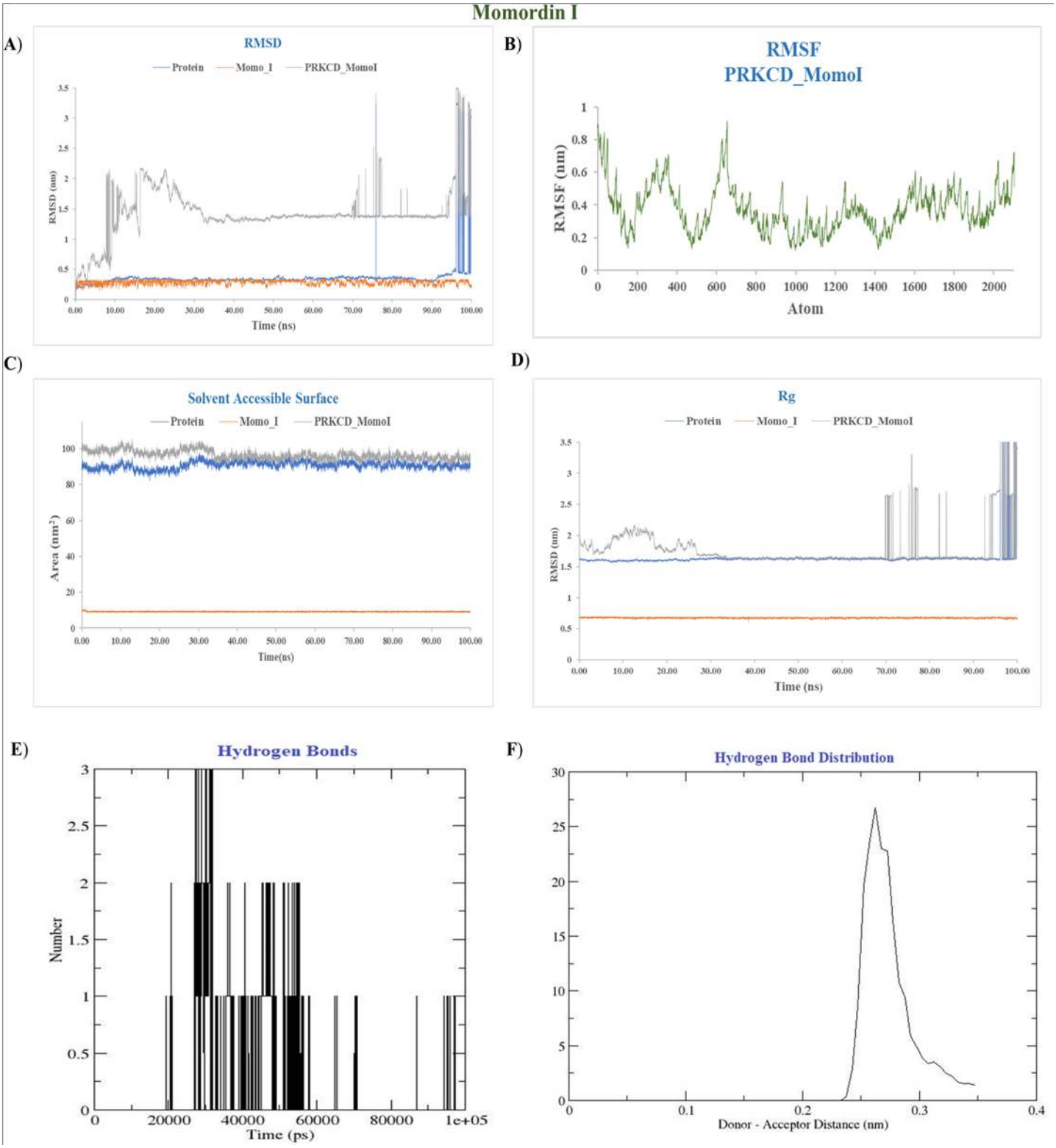


Figure 7

PRKCD interactions with the Momordin I, monitored during the 100 ns of simulation **A)** RMSD value (Protein: Blue, Momordin I: Orang, Complex: Grey), **B)** RMSF of Complex **C)** SASA value (Protein: Blue, Momordin I: Orang, Complex: Grey) **D)** Rg (Protein: Blue, Momordin I: Orang, Complex: Grey) **E)** Number of H-bond **F)** Hydrogen bond distribution

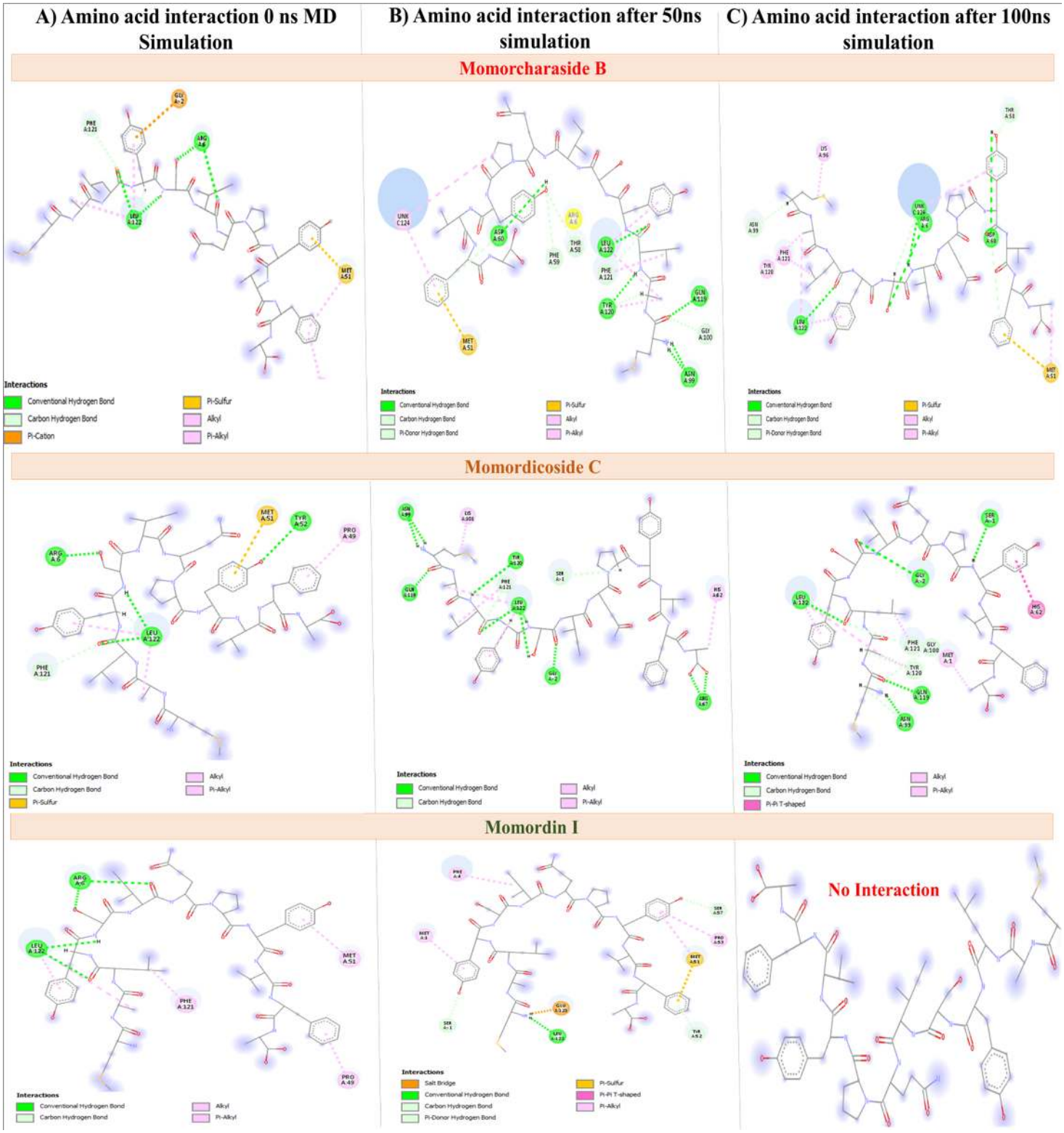


Figure 8

2D Amino acid interaction during of Momorcharaside B, Momordicoside C and Momordin I during MD Simulation **A)**Interaction at 0ns **B)** Interaction at 50ns **C)** Interaction at 100ns

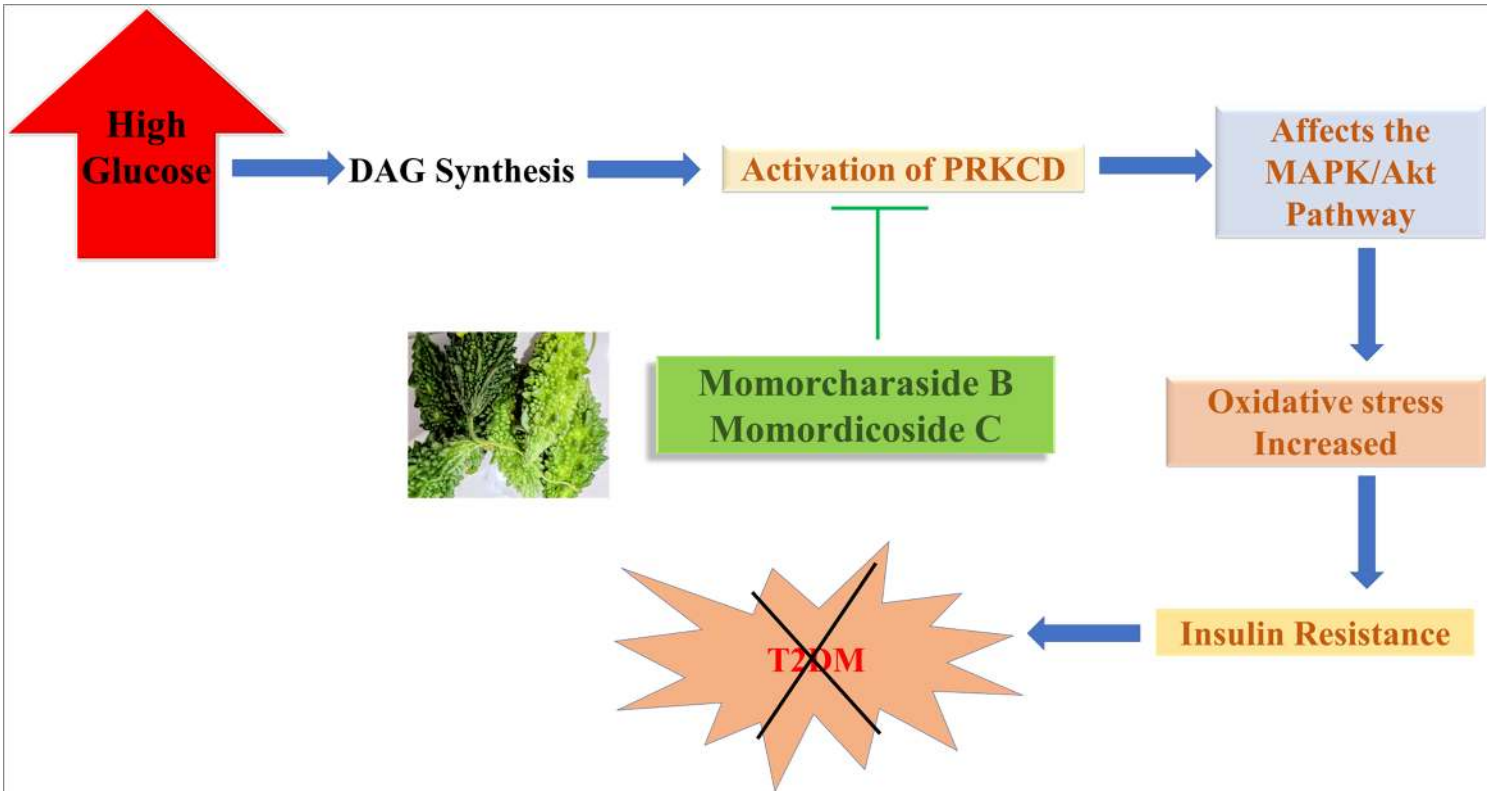


Figure 9

Proposed mechanism action of Momorcharaside B and Momordicoside C targeting PRKCD

Supplementary Files

This is a list of supplementary files associated with this preprint. Click to download.

- Table1.docx